

RT-GAN: Recurrent Temporal GAN for Adding Lightweight Temporal Consistency to Frame-Based Domain Translation Approaches

Shawn Mathew*, Saad Nadeem*, Alvin C. Goh, and Arie Kaufman, *Fellow, IEEE*

Abstract—While developing new unsupervised domain translation methods for endoscopy videos, it is typical to start with approaches that initially work for individual frames without temporal consistency. Once an individual-frame model has been finalized, additional contiguous frames are added with a modified deep learning architecture to train a new model for temporal consistency. This transition to temporally-consistent deep learning models, however, requires significantly more computational and memory resources for training. In this paper, we present a lightweight solution with a tunable temporal parameter, RT-GAN (Recurrent Temporal GAN), for adding temporal consistency to individual frame-based approaches that reduces training requirements by a factor of 5. We demonstrate the effectiveness of our approach on two challenging use cases in colonoscopy: haustral fold segmentation (indicative of missed surface) and realistic colonoscopy simulator video generation. The datasets, accompanying code, and pretrained models will be made available at <https://github.com/nadeemlab/CEP>.

Index Terms—Colonoscopy, domain translation, generative-adversarial networks, temporal consistency, video-to-video translation.

I. INTRODUCTION

The video modality has become more and more commonplace in medical tasks and procedures as cameras provide eyes for the doctors and other instrument guidance systems. Processing these video sequences in realtime can provide new tools to assist doctors during their procedures and patient care. As more procedures and tools bring cameras into the workflow, new interesting and innovative tasks arise. When tackling new tasks that process video sequences it is quite natural to begin by breaking the problem down into frames. For tasks such as segmentation and depth inference, where a single correct answer can be predicted from the image, individually processed frames can be stitched together to produce adequate results. Realistic video generation, on the other hand, requires certain elements such as textures and geometry to be consistent between frames. Frame-by-frame processing in this case, would produce flickery results. These problems require components to provide temporal consistency

between frames. Providing these temporal components require additional overhead in both the development time and resources.

Recently, unsupervised domain translation methods have shown promising results across different endoscopy tasks, but not all have been extended to video. The domain translation models that have been extended to video create new models from scratch to accommodate video sequences. Once a frame-based model has been finalized, one can either try simple post-processing normalization across frames to get “quasi-consistency” [18] or train a new model from scratch with full temporal consistency. The first approach is only possible on very specific tasks, such as depth estimation, where there is one correct result. Tasks such as realistic image generation cannot be concatenated together with simple approaches. The second, more general option however requires significantly more computational and memory resources for training.

Moreover, temporally-consistent unsupervised video-to-video domain translation (RecycleGAN [1] derivatives) typically requires learning both directions of translation when only a single direction may be relevant, for example, colonoscopy to depth, colonoscopy to fold segmentation, synthetic to real colonoscopy simulation, etc. This forward and backward learning with temporal components increases the number of learnable parameters by several orders of magnitude. Even still, the general approaches like RecycleGAN may not utilize domain specific knowledge that can vastly improve results. In this work, we present Recurrent Temporal Generative-Adversarial Network (RT-GAN) for adding lightweight temporal-consistency to unsupervised image-to-image domain translation models (that reduces training requirements by a factor of 5). RT-GAN allows traversal between temporal consistency and fidelity to the frame-based models using a single tunable weight parameter while focusing on a single translation direction. Specifically, RT-GAN uses recurrent information by referencing the previous frame and its result as seen in Figure 1c. A temporal discriminator takes the generator’s results for 3 consecutive frames to build temporal consistency. A recent approach, RAVE [7], also uses recurrent generators for video domain translation, but needs to be trained from scratch. Frame-based domain translation models can learn useful representations with task-specific components (priors, losses, etc) but these components need to be redesigned or dropped altogether when transitioning to a new unsupervised video-to-video domain translation model such as RAVE. In contrast, RT-GAN builds on the representations learned by any

This project was supported by MSK Cancer Center Support Grant/Core Grant (P30 CA008748) and NSF grants OAC1919752, ICER1940302, and IIS2107224. ***First two authors contributed equally.**

S. Mathew and A. Kaufman are with Department of Computer Science, Stony Brook University, Stony Brook, NY 11794-2424, USA. (e-mail: [shawnmathew,ari]@cs.stonybrook.edu).

S. Nadeem is with the Department of Medical Physics and A.C. Goh is with the Department of Surgery, Memorial Sloan Kettering Cancer Center, New York, NY 10065. (email: [nadeems,goha]@mskcc.org).

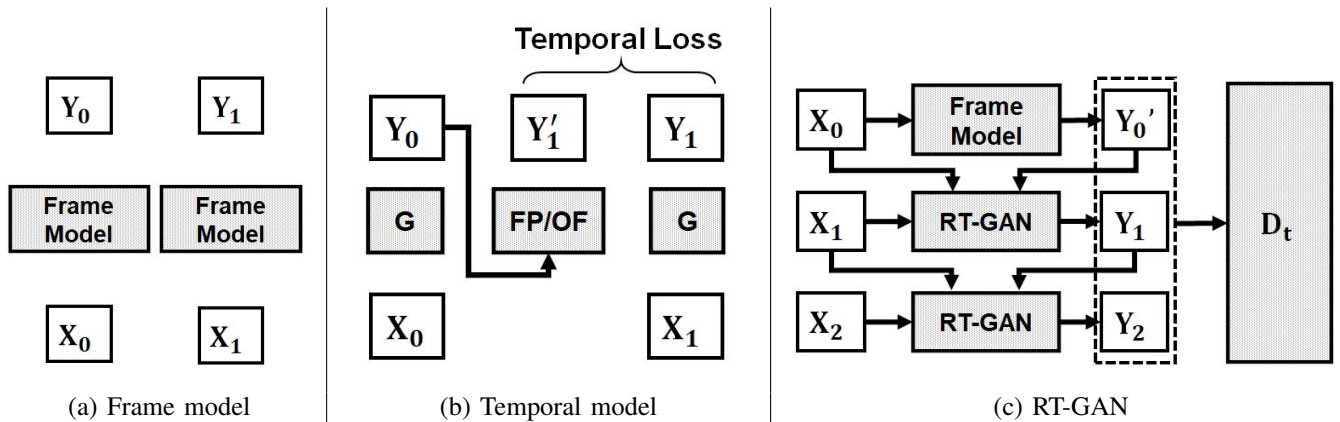


Fig. 1. Depicting how temporal consistency can be added. X is the input video and Y is the resulting video output. (a) Depicts the case where each frame is processed individually by a frame-based model. These results can be jittery without temporal consistency. (b) Shows one way that temporal consistency is added to models such as RecycleGAN [1] and OfGAN [33]. An optical flow module or deep learning frame predictor is used to predict the next frame from the current frame. These additional modules require more resources for training. (c) Illustrates RT-GAN adversarial approach to temporal consistency. RT-GAN references the previous frame and its output to translate the current frame. Three consecutive output frames from generators are passed into a discriminator to provide temporal consistency. The first frame, Y'_0 is generated from a fully trained frame-based model. The other two frames are created by RT-GAN to be temporally consistent with Y'_0 .

unsupervised image-to-image domain translation model and adds temporal consistency to these without needing to redesign task-specific components. We demonstrate the effectiveness of RT-GAN in adding lightweight temporal consistency to two frame-based models, FoldIt [16] haustal fold segmentation model with some inherent “quasi-consistency” across frames and CLTS-GAN color-lighting-texture-specular reflection augmentation model with no consistency at all across frames.

The contributions of this work are as follows:

- 1) A method to add temporal consistency to established frame-based models
- 2) An efficient and less resource-hungry method for video domain translation
- 3) A tunable way to control the trade off between temporal smoothness and faithfulness to the frame-based model
- 4) Demonstrate the effectiveness of RT-GAN in two challenging use cases: haustal fold segmentation (indicative of missed surface) and real colonoscopy video simulation.

II. RELATED WORKS

Generative Adversarial Networks (GANs) [8] proposed image generation using adversarial learning. GANs use two networks, one to generate images and one to learn the differences between the dataset and generated images. Many different variations and use cases of GANs were created to solve a number of different tasks including face generation [10], [13], [29], segmentation [5], [12], [23], future frame prediction [11], [24] and more. The adversarial learning approach has also shown to be useful in video generation tasks [27], [30], [35].

Domain translation is the task of translating a sample from one domain to another. Pix2Pix [9] is a network that provides a solution for supervised image-to-image domain translation. Pix2pix used conditional GANs [19] with an L1 loss to tackle but it requires ground truth/paired information. In contrast, CycleGAN [36] presented a method for unsupervised/unpaired

domain translation using a cycle consistency loss for forward and backward translation between two given domains. A number of follow-up works have adopted this cycle consistency loss or variations of it for task-specific frame-based image-to-image domain translation models [11], [16], [34]. The task-specific components in these frame-based models are critical for obtaining best results but these need to be redesigned or dropped altogether when transitioning to a completely new video-to-video domain translation model.

Similar to image-to-image-domain translations, there are video-to-video domain translation that require ground truth annotations [31], [32]. Bashkirova et al. performed a number of experiments using a CycleGAN model that uses 3D convolutions with varying input types such as randomly sorted frames, ordered frames, and frames stacked as a 3D tensor. They found that using the stacking frames into 3D tensors provided the best results at the cost of extra training requirements [2]. Bansal et al. proposed RecycleGAN [1], a network for unsupervised video retargeting, that does not require any task-specific modules and adds temporal consistency components (such as optical flow) on CycleGAN to extend it to videos (Figure 1b). Specifically, an additional future frame prediction network is added for temporal consistency. This increases memory requirements especially since two predictor networks are needed, one for each domain. OfGAN [33] predicts optical flow using an architecture similar to the one shown in Figure 1b to translate synthetic colonoscopy sequences to real colonoscopy video sequences; OfGAN relies on texture, lighting, and specular reflection information to be embedded in the input videos to generate realistic colored output sequences. MocalypseGAN [3], similar to OfGAN, estimates optical flow for unsupervised video domain translation for more general tasks. Chu et al. [4] presented UVT that used an additional network to warp frames for temporal consistency, similar to the next frame predictor network. A more recent work, RAVE [7], provides real-time video domain translation using a recurrent

generator. RAVE’s generator applies an adversarial loss to learn temporal consistency similar to our work (Figure 1c) but needs to be trained from scratch while requiring modifications of domain-specific components for new problems.

III. DATASET

The OC and VC dataset was created from 10 patients that had VC procedures followed by OC procedures. The OC videos were cropped to a size of 256x256 to remove borders in the frames created by the fish-eye lens in the colonoscope. The videos for VC were created from triangulated meshes of the colon extracted from CT scans as described by Nadeem et al. [20]. A virtual camera flies through the mesh with random rotations and lights at both sides of the camera. To better replicate the conditions of the colonoscopy procedure, the inverse square fall-off property is applied to the lights [15]. The videos for both the VC and OC datasets were split into 300 sets of 3 sequential frames. In total, training dataset is composed of 1500 frame triplets, while the validation and testing datasets were composed of 900 and 600 frame triplets respectively. Haustral fold segmentation data is generated in a similar manner to Mathew et al. [16].

IV. METHODS

Typically for unsupervised domain translation, at least 2 generator networks are being updated during training time. One generator learns the translation between the input domain and output domain, while the other learns the inverse direction. Typically, applications only require one generator to provide the domain translation results. RT-GAN only trains one generator reducing resources during training (see Table I). RT-GAN builds off of the results from a fully trained frame-based model, F . The results of the frame-based model can be pre-computed, so it does not affect the required resources for training. The RT-GAN’s generator G , translates from the input domain X to the output domain Y . G takes 3 images as input to produce the output y'_t . The first input is the frame, x_t that is to be translated. The next input is the previous frame in the input sequence, x_{t-1} , to give the network context and a better understanding of motion. The last input image for G is y'_{t-1} , the result for x_{t-1} . y'_{t-1} gives the generator context on the previous frame with which the output needs to be temporally consistent with. The input for RT-GAN’s generator can be seen in Figure 1c.

G is trained using two discriminators, each having its own adversarial loss. The adversarial loss described below:

$$\mathcal{L}_{adv}(G, D, y, y') = \log(D(y)) + \log(1 - D(y')), \quad (1)$$

where y' is from the generator and y is from the training data.

The first discriminator, D_t , learns temporal consistency. D_t compares a 3 frame sequence from the output domain to a 3 frame sequence created from the generators. The first frame in the triplet is provided by F , while the next 2 temporally consistent frames are provided by G . G aligns its results with F in order to provide temporal consistency, but F ’s results is

TABLE I

THE NUMBER OF LEARNABLE PARAMETERS (IN MILLIONS) AND THE TIME IT TAKES TO TRAIN ONE EPOCH FOR RECYCLEGAN [1], TEMP CYCLEGAN [6], FOLDIT [16], CLTS-GAN [17], AND RT-GAN (OURS). RT-GAN REDUCES THE NUMBER OF LEARNABLE PARAMETERS BY A FACTOR OF 5 WHEN COMPARED WITH RECYCLEGAN WHILE DECREASING TRAINING TIME ALMOST IN HALF. RECYCLEGAN NEEDS TO LEARN TWO DIRECTIONS OF TRANSLATION IN ADDITION TO ITS TEMPORAL CONSISTENCY MODULES. TEMP CYCLEGAN NEEDS TWICE AS LONG AND TWICE THE MEMORY DURING TRAINING. FOLDIT NEEDS TO LEARN FOUR DIRECTIONS OF TRANSLATION, WHILE CLTS-GAN ONLY NEEDS TWO. RT-GAN ONLY LEARNS ONE DIRECTION WHICH SHOWS SIGNIFICANT IMPROVEMENT OVER THE OTHER MODELS. THESE MODELS WERE TRAINED ON AN NVIDIA QUADRO RTX 6000 GPU.

	Learnable Parameters	Epoch Training Time
RecycleGAN	137.11	~ 742 s
TempCycleGAN	46.65	~ 836 s
Foldit	82.14	~ 700 s
CLTS-GAN	55.15	~ 857 s
RT-GAN	25.22	~ 394 s

independent of G . The temporal adversarial loss is described as,

$$\mathcal{L}_t(G, F, D_t, Y, X) = \mathcal{L}_{adv}(G, D_t, \{y_0, y_1, y_2\}, \{F(x_0), y'_1, y'_2\}), \quad (2)$$

where y'_1 is $G(x_0, x_1, F(x_1))$ and y'_2 is $G(x_1, x_2, y'_1)$.

A separate discriminator, D_f , ensures that G ’s results appear similar to F . It compares the paired input and output frames for F and G . The adversarial loss for D_f is described as:

$$\mathcal{L}_f(G, F, D_f, X) = \mathcal{L}_{adv}(G, D_f, \{x_1, F(x_1)\}, \{x_1, y'_1\}) \quad (3)$$

A stationary loss, \mathcal{L}_s is included to add extra stability to the model. When the camera is stationary the output should remain the same. This is simulated in the stationary loss and is defined as:

$$\mathcal{L}_s(G, X) = \|y'_1 - G(x_1, x_1, y'_1)\|_1, \quad (4)$$

where $\|\cdot\|$ represents the ℓ_1 norm.

The complete objective function for the network is:

$$\mathcal{L}_{obj} = \lambda \mathcal{L}_t(G, F, D_t, Y, X) + \mathcal{L}_f(G, F, D_f, X) + \mathcal{L}_s(G, X) \quad (5)$$

where λ is a tunable weight to determine the tradeoff between the temporal smoothness and fidelity to the frame-based model. D_t is a PatchGAN discriminator with 3D convolutions to help it learn temporal information while D_f is a PatchGAN discriminator with 2D convolutions to learn spatial information. G uses a Resnet architecture with 9 blocks.

V. RESULTS

The training time and memory usage of RT-GAN is analyzed in Table I. RT-GAN reduces the number of learnable parameters by a factor of 5 while decreasing the training time when compared with RecycleGAN. Compared the TempCycleGAN, a video domain translation model with a minimal amount of image generators, RT-GAN reduces the number of learnable parameters and training time by a factor of 2. FoldIt, a frame-based model for haustral fold segmentation, uses

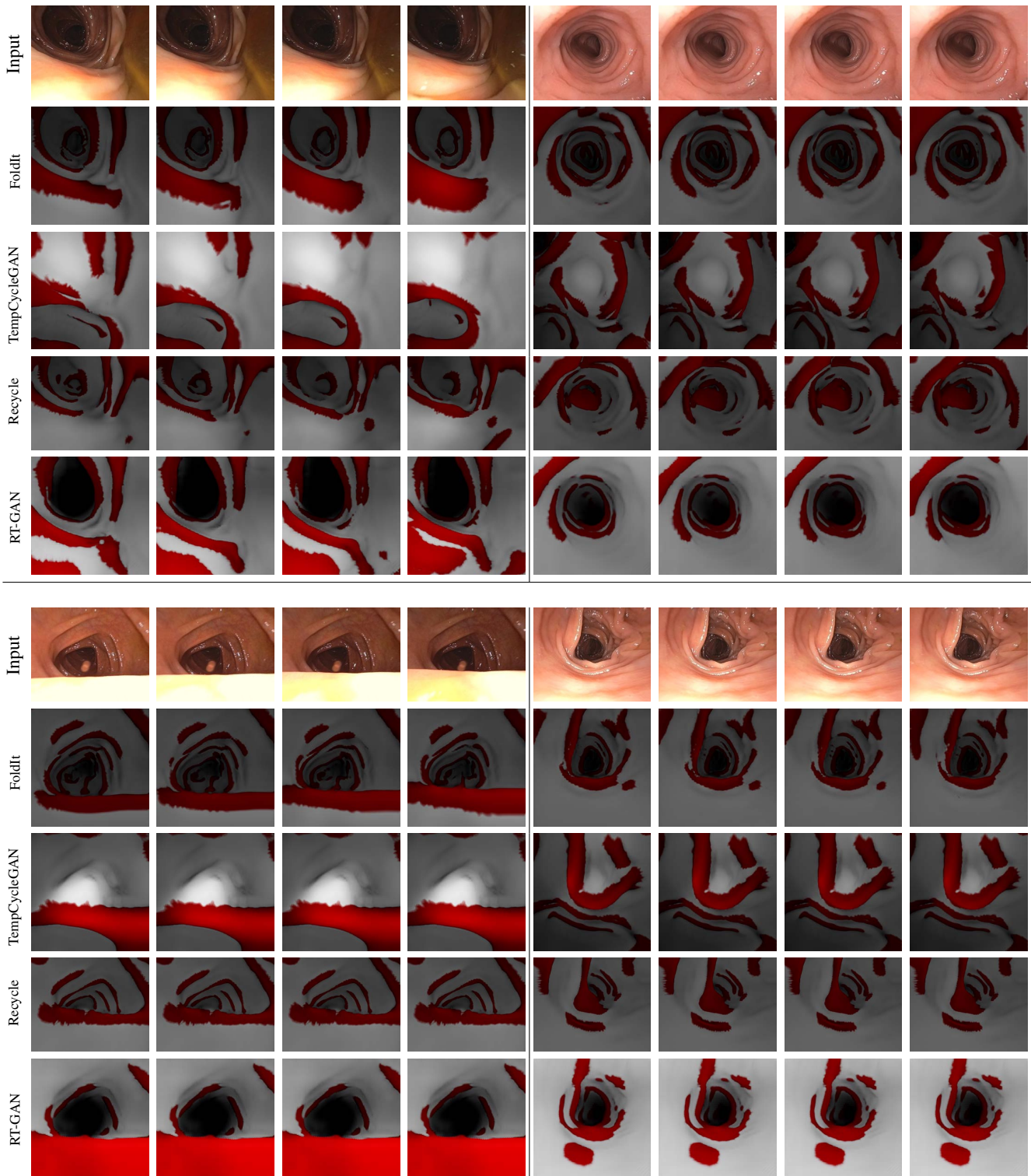


Fig. 2. Comparisons of the results for RT-GAN with stitched images from FoldIt and RecycleGAN. The first row shows the optical colonoscopy frames from [14] while the second row shows FoldIt’s results. FoldIt shows a bit of jitteriness, and in the first sequence the deeper parts of the colon gets smoothed out. The third row shows TempCycleGAN, which is unable to properly handle the depth and the deeper parts of the colon. RecycleGAN is displayed in the fourth row. On the right sequences, the model marks deeper parts of the colon as folds due to the lack of task specific modules. The last row shows RT-GAN results that are smoother and maintain the depth of the colon in its output. Full results are found in the **supplementary video**.

fewer resources than RecycleGAN as it deals with individual frames. RT-GAN still requires lesser resources than FoldIt because it only learns one direction of translation while FoldIt learns four [16]. CLTS-GAN [17] only learns two directions

of translation, so RT-GAN reduces the learnable parameters in half. When training RT-GAN, the hardware requirements are capped by the frame-based model since RT-GAN requires lesser resources. To get an intuition of the computa-



Fig. 3. Haustral fold segmentation results on a synthetic colon with two different textures. The first two rows show the input followed by the ground truth annotations. The following rows show the results for RecycleGAN, FoldIt and RT-GAN. The result videos can be found in the **supplementary video**.

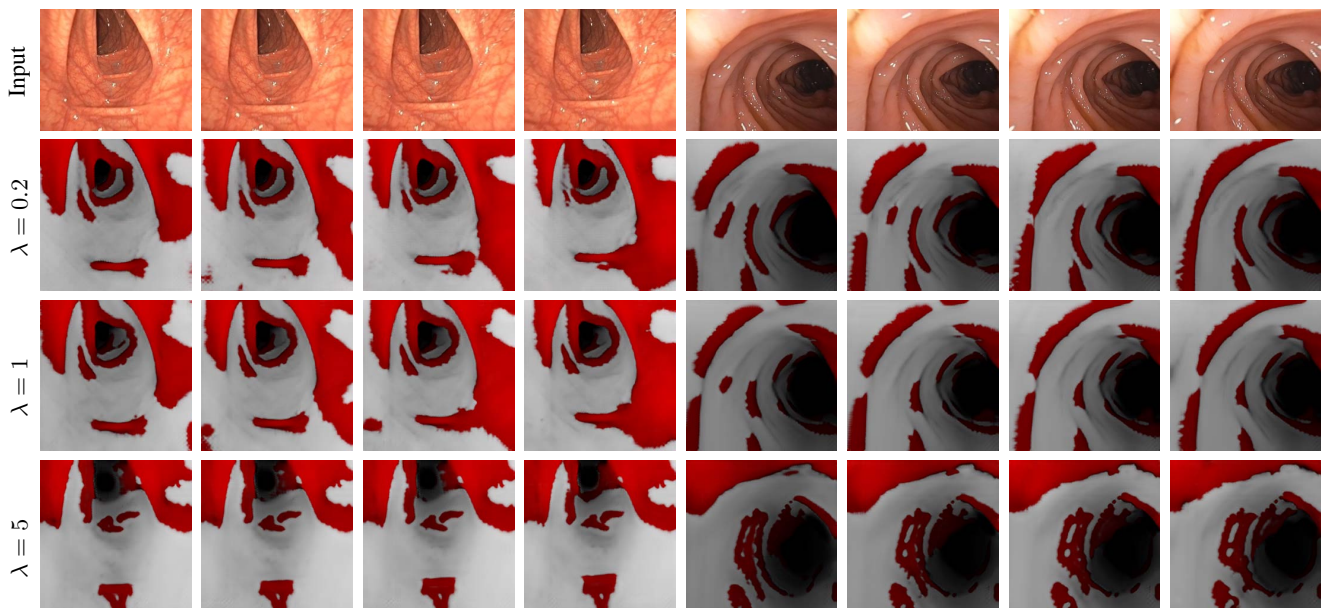


Fig. 4. Results for varying temporal weights (λ). The first row is the input and the second row shows $\lambda = 0.2$. As λ decreases RT-GAN’s is more faithful to FoldIt. The next row shows $\lambda = 1$ where there is a balance between temporal and the frame losses. The last row shows $\lambda = 5$. Here the annotation shapes tend to remain consistent between frames. Full videos are found in the **supplementary material**.

tional/memory training resources for video domain translation approaches in colonoscopy, OfGAN [33] (the colonoscopy simulator model) used 4 GPUs with 16 GB each for training whereas RT-GAN was trained on a single 24 GB GPU.

To test the effectiveness of RT-GAN in fold segmentation context (indicative of the total missed surface during colonoscopy), we added RT-GAN on top of FoldIt haustral fold frame-based model [16]. In Figure 2, we compare RT-GAN, FoldIt, TempCycleGAN, and RecycleGAN results on public video sequences from Ma et al. [14]. RecycleGAN has many variants, however sifting through all the variants and applying task-specific components requires great effort on part of the end users. We chose RecycleGAN for comparisons since it has all the base temporal components seen in the more advanced variants and is not task-specific. We also compare with TempCycleGAN which has shown results on medical tasks. FoldIt and RecycleGAN both had jittery results. FoldIt occasionally smooths out the deeper parts of the endolumen. In contrast, RecycleGAN translated these deeper endolumen parts as folds since it does not contain any task-specific modules or losses. RT-GAN utilizes the task-specific modules from FoldIt while providing temporal consistency. TempCycleGAN is more consistent, however, similar to RecycleGAN it doesn’t have the task specific additions and it fails to accommodate the deeper portions of the endoluminal view. The complete videos for these results can be seen in the **supplementary video**.

For quantitative analysis, a synthetic colon with ground truth annotations is rendered using two different textures, similar to [16]. Table II shows that RT-GAN’s additional temporal consistency provided improvement on the IoU and DICE scores for both textures. RT-GAN is also more consistent than the other models despite different textures. Additionally, the

TABLE II
QUANTITATIVE RESULTS FOR HAUSTRAL FOLD SEGMENTATION ON A SYNTHETIC COLON WITH TWO TEXTURES AND GROUND TRUTH FOLD ANNOTATIONS (COMPUTED USING [21]). RT-GAN HAS BETTER IOU AND DICE SCORES FOR BOTH TEXTURED COLONS. THE CONSISTENCY COLUMN INDICATES THE FRAME-BASED GEOMETRIC CONSISTENCY OF THE MODEL DESPITE DIFFERENT TEXTURES AS DESCRIBED BY MATHEW ET AL. [18]. THESE SEQUENCES ARE SHOWN IN THE SUPPLEMENTARY MATERIAL.

		Texture 1	Texture 2	Consistency [18]
Dice	RecycleGAN	0.34	0.33	0.76
	FoldIt	0.47	0.50	0.77
	RT-GAN	0.55	0.54	0.81
IoU	RecycleGAN	0.21	0.20	0.63
	FoldIt	0.31	0.33	0.64
	RT-GAN	0.39	0.38	0.69

optical flow can be compared between in the input sequences and output sequences as done by Rivoir et al. [25]. The mean difference between the input optical flow and output optical flow on our textured colons for RecycleGAN, FoldIt, and RT-GAN are 2.4788, 0.9021, and 0.8479, respectively. This indicates that RT-GAN is better capable of capturing to motion between frames when compared with other models like RecycleGAN and FoldIt. The synthetic colon results can be found in Figure 3. In Figure 4, the λ parameter to control temporal consistency is shown. When λ is set to a lower value, it tries to be more faithful to FoldIt. As λ is increased, RT-GAN makes the annotations smoother so it looks more temporally consistent.

We evaluated RT-GAN on real colonoscopy video generation/simulation using the frame-based CLTS-GAN model [17]. CLTS-GAN creates colonoscopy frames with different colors, lighting, textures, and specular reflections using noise parameters. For real colonoscopy video generation/simulation, RT-GAN was trained for 200 epochs on 1800 frame triplets

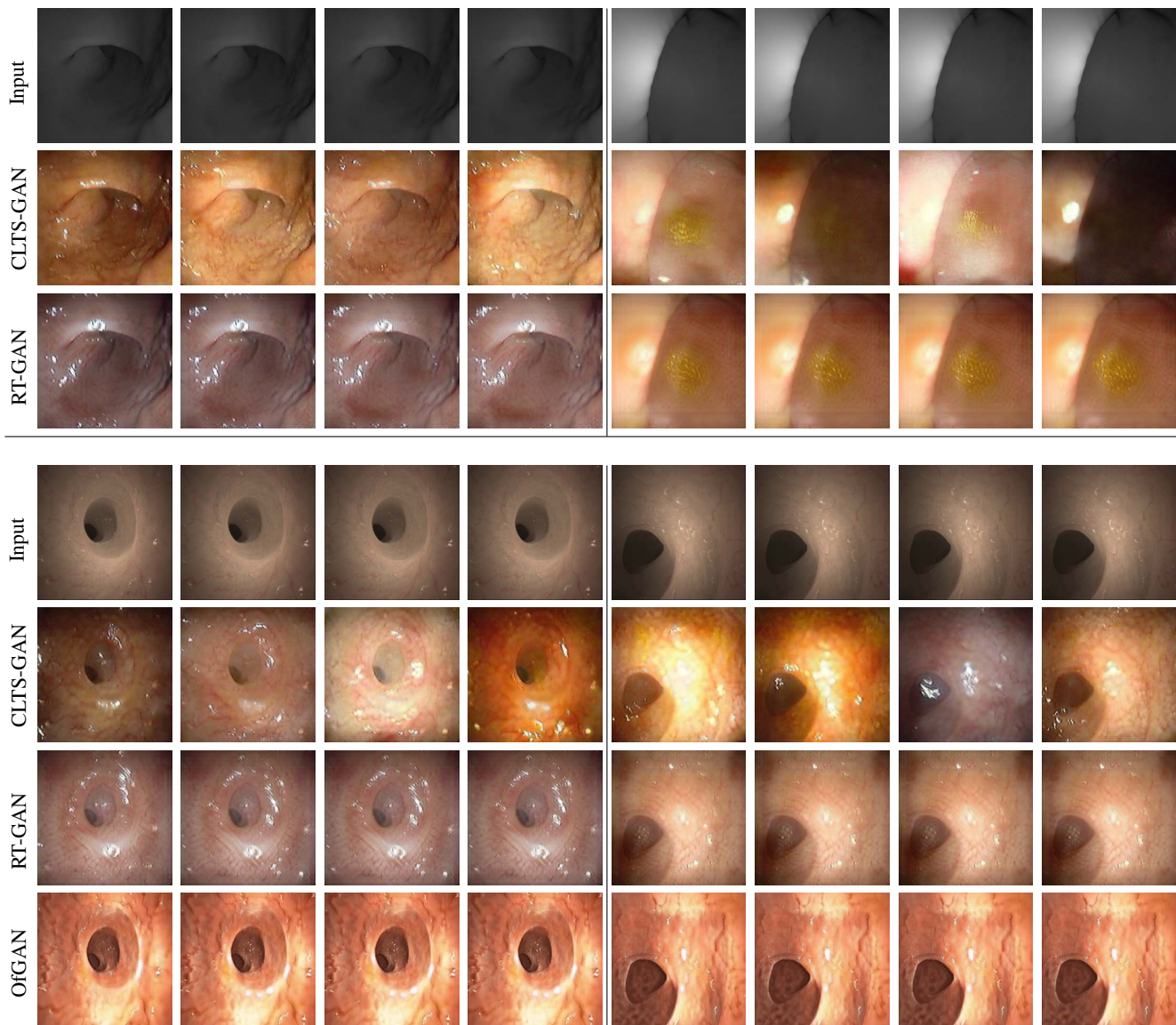


Fig. 5. Results for RT-GAN trained on CLTS-GAN. The top portion shows results on rendered mesh frames. CLTS-GAN’s results change drastically over time. RT-GAN builds off CLTS-GAN to provide consistent specular and texture between frames. The bottom half shows results using OfGAN’s input video, which embeds texture and specular information. CLTS-GAN adds more intricate specular reflections and textures, and RT-GAN inherits this property. OfGAN relies on the embedded texture and specular to produce its output. Full videos are in the **supplementary video**.

of colonoscopy video and 3D renderings of the colon using virtual colonoscopy from [17]. The results of real colonoscopy video generation from synthetic sequences are shown in Figure 5. The top half shows video generation from virtual colonoscopy renderings. CLTS-GAN’s use of noise parameters allows it to generate drastically different output across frames. RT-GAN is much smoother and the specular reflections and textures are consistent; in the **supplementary video**, the overall color and lighting changes over time since RT-GAN only looks at the previous frame (and doesn’t have a longer-term memory, an issue we will resolve in the future). The bottom portion of Figure 5 compares (RT-GAN + CLTS-GAN) with OfGAN [33]. OfGAN is confined to creating textures and specular reflections that are embedded in its input video. In contrast, CLTS-GAN adds additional texture and specular reflections but lacks temporal consistency. RT-GAN uses CLTS-

GAN’s texture and specular information and adds temporal consistency on top of it. Full videos of the colonoscopy video generation results are in the **supplementary video**.

VI. CONCLUSION AND FUTURE WORK

In this paper, we presented a new method, RT-GAN, to add temporal consistency to established frame-based models. This is an efficient and considerably less resource-hungry method for video domain translation. RT-GAN also provides a tunable way to control the trade off between temporal smoothness and faithfulness to the frame-based model. We demonstrate the effectiveness of RT-GAN in two challenging use cases: haustral fold segmentation (indicative of missed surface) and real colonoscopy video simulation.

There are two general failure cases for RT-GAN that can be seen in Figure 6. The first failure case is the lack of long

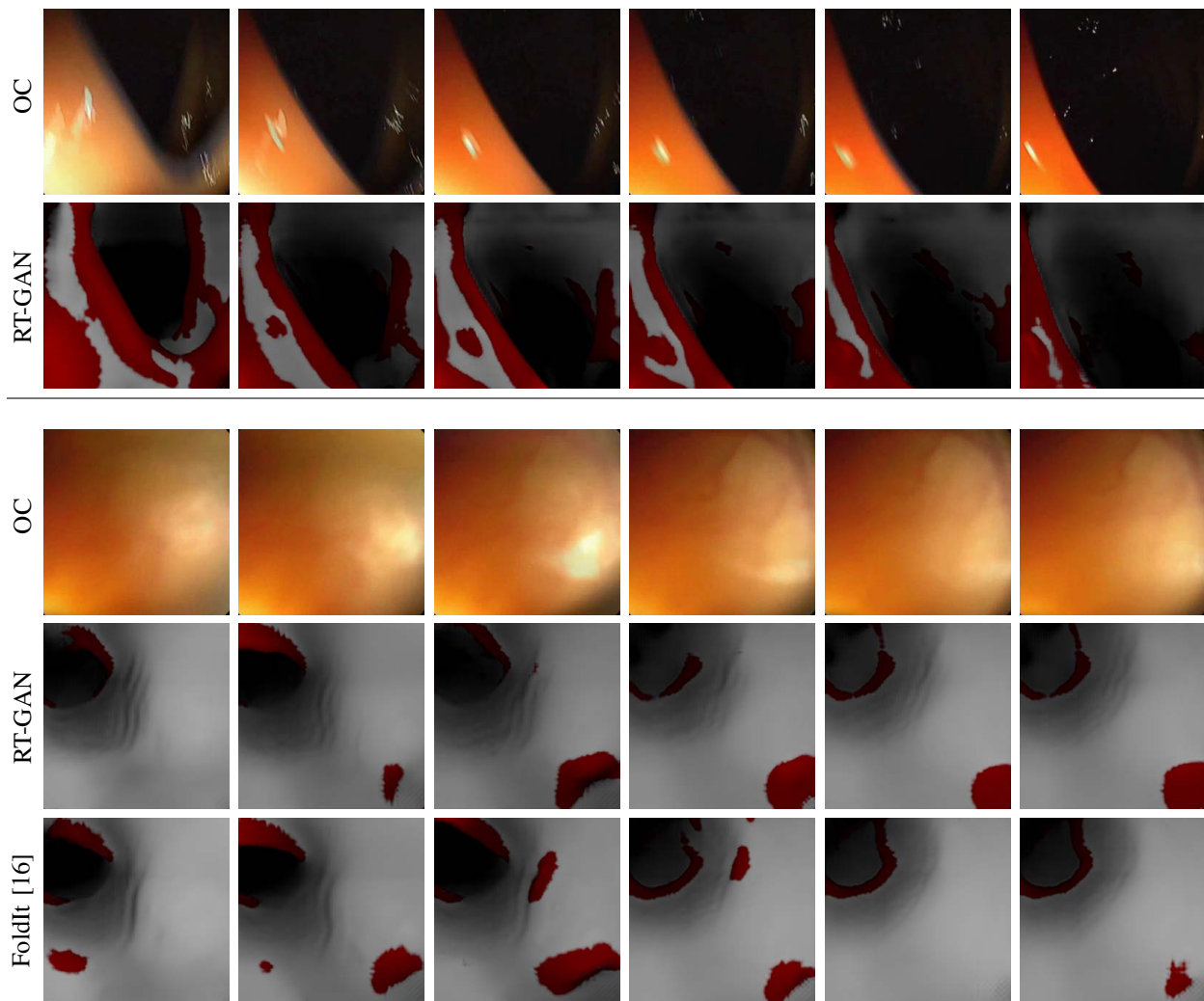


Fig. 6. Failure cases for RT-GAN. In the sequence above, the folds deeper in the colon appear to fade along with the annotation as RT-GAN does not have any long term temporal consistency. The second sequence shows a sequence of frames where the camera is occluded, but there are annotations. Similarly, FoldIt shows similar results. RT-GAN relies on the frame based model making it so they share some failure cases.

term memory, which is shown in the top portion of Figure 6. The deeper parts of the colon that are annotated in the first few frames disappear in the later frames. This is due to the fact that RT-GAN only receives information from the previous frame. Information about the deeper parts of the colon from earlier frames get lost. A similar effect is seen in the global drift when RT-GAN generates realistic colonoscopy video sequences. Long term memory or transformer components from models like [7], [22], [26], [28] could mitigate this issue. Additionally, RT-GAN can inherit some of the limitations of its frame based model. In the bottom portion of Figure 6, one of the failure cases for FoldIt is displayed. FoldIt cannot handle frame occlusion and hence both FoldIt and RT-GAN can hallucinate endoluminal view for occluded frames. Going forward, we plan to try RT-GAN on non-colonoscopy datasets such as the AdaptOR Challenge dataset for mitral valve repair simulation (unsupervised video-to-video domain translation task) to show how it can be applied to other tasks [6].

REFERENCES

- [1] Bansal, A., Ma, S., Ramanan, D., Sheikh, Y.: Recycle-gan: Unsupervised video retargeting. *Proceedings of the European Conference on Computer Vision (ECCV)* pp. 119–135 (2018)
- [2] Bashkirova, D., Usman, B., Saenko, K.: Unsupervised video-to-video translation. *arXiv preprint arXiv:1806.03698* (2018)
- [3] Chen, Y., Pan, Y., Yao, T., Tian, X., Mei, T.: Mocycle-gan: Unpaired video-to-video translation. *Proceedings of the 27th ACM International Conference on Multimedia* pp. 647–655 (2019)
- [4] Chu, M., Xie, Y., Mayer, J., Leal-Taixé, L., Thurey, N.: Learning temporal coherence via self-supervision for gan-based video generation. *ACM Transactions on Graphics (TOG)* **39**(4), 75–1 (2020)
- [5] Dong, X., Lei, Y., Wang, T., Thomas, M., Tang, L., Curran, W.J., Liu, T., Yang, X.: Automatic multiorgan segmentation in thorax CT images using u-net-gan. *Medical Physics* **46**(5), 2157–2168 (2019)
- [6] Engelhardt, S., De Simone, R., Full, P.M., Karck, M., Wolf, I.: Improving surgical training phantoms by hyperrealism: deep unpaired image-to-image translation from real surgeries. *International Conference on Medical Image Computing and Computer-Assisted Intervention (MICCAI)* pp. 747–755 (2018)
- [7] Fuoli, D., Huang, Z., Paudel, D.P., Van Gool, L., Timofte, R.: An efficient recurrent adversarial framework for unsupervised real-time video enhancement. *International Journal of Computer Vision* pp. 1–18 (2023)
- [8] Goodfellow, I., Pouget-Abadie, J., Mirza, M., Xu, B., Warde-Farley, D., Ozair, S., Courville, A., Bengio, Y.: Generative adversarial nets.

- Advances in Neural Information Processing Systems. pp. 2672–2680 (2014)
- [9] Isola, P., Zhu, J.Y., Zhou, T., Efros, A.A.: Image-to-image translation with conditional adversarial networks. *Proceedings of the IEEE Conference on Computer Vision and Pattern Recognition (CVPR)* pp. 1125–1134 (2017)
- [10] Karras, T., Laine, S., Aila, T.: A style-based generator architecture for generative adversarial networks. *Proceedings of the IEEE/CVF Conference on Computer Vision and Pattern Recognition (CVPR)* pp. 4401–4410 (2019)
- [11] Kwon, Y.H., Park, M.G.: Predicting future frames using retrospective cycle gan. *Proceedings of the IEEE/CVF Conference on Computer Vision and Pattern Recognition (CVPR)* pp. 1811–1820 (2019)
- [12] Liu, K., Ye, Z., Guo, H., Cao, D., Chen, L., Wang, F.Y.: Fiss gan: A generative adversarial network for foggy image semantic segmentation. *IEEE/CAA Journal of Automatica Sinica* **8**(8), 1428–1439 (2021)
- [13] Liu, M., Li, Q., Qin, Z., Zhang, G., Wan, P., Zheng, W.: Blendgan: Implicitly gan blending for arbitrary stylized face generation. *Advances in Neural Information Processing Systems* **34**, 29710–29722 (2021)
- [14] Ma, R., Wang, R., Pizer, S., Rosenman, J., McGill, S.K., Frahm, J.M.: Real-time 3D reconstruction of colonoscopic surfaces for determining missing regions. *International Conference on Medical Image Computing and Computer-Assisted Intervention (MICCAI)* pp. 573–582 (2019)
- [15] Mahmood, F., Chen, R., Durr, N.J.: Unsupervised reverse domain adaptation for synthetic medical images via adversarial training. *IEEE Transactions on Medical Imaging* **37**(12), 2572–2581 (2018)
- [16] Mathew, S., Nadeem, S., Kaufman, A.: Foldit: Haustral folds detection and segmentation in colonoscopy videos. *International Conference on Medical Image Computing and Computer-Assisted Intervention (MICCAI)* pp. 221–230 (2021)
- [17] Mathew, S., Nadeem, S., Kaufman, A.: CLTS-GAN: color-lighting-texture-specular reflection augmentation for colonoscopy. *International Conference on Medical Image Computing and Computer-Assisted Intervention (MICCAI)* pp. 519–529 (2022)
- [18] Mathew, S., Nadeem, S., Kumari, S., Kaufman, A.: Augmenting colonoscopy using extended and directional CycleGAN for lossy image translation. *Proceedings of the IEEE/CVF Conference on Computer Vision and Pattern Recognition (CVPR)* pp. 4696–4705 (2020)
- [19] Mirza, M., Osindero, S.: Conditional generative adversarial nets. *arXiv preprint arXiv:1411.1784* (2014)
- [20] Nadeem, S., Kaufman, A.: Computer-aided detection of polyps in optical colonoscopy images. *SPIE Medical Imaging* **9785**, 978525 (2016)
- [21] Nadeem, S., Marino, J., Gu, X., Kaufman, A.: Corresponding supine and prone colon visualization using eigenfunction analysis and fold modeling. *IEEE Transactions on Visualization and Computer Graphics* **23**(1), 751–760 (2016)
- [22] Neimark, D., Bar, O., Zohar, M., Asselmann, D.: Video transformer network. *Proceedings of the IEEE/CVF International Conference on Computer Vision (ICCV)* pp. 3163–3172 (2021)
- [23] Nema, S., Dudhane, A., Murala, S., Naidu, S.: RescueNet: an unpaired gan for brain tumor segmentation. *Biomedical Signal Processing and Control* **55**, 101641 (2020)
- [24] Nguyen, K.T., Dinh, D.T., Do, M.N., Tran, M.T.: Anomaly detection in traffic surveillance videos with gan-based future frame prediction. *Proceedings of the International Conference on Multimedia Retrieval* pp. 457–463 (2020)
- [25] Rivoir, D., Pfeiffer, M., Docea, R., Kolbinger, F., Riediger, C., Weitz, J., Speidel, S.: Long-term temporally consistent unpaired video translation from simulated surgical 3D data. *Proceedings of the IEEE/CVF International Conference on Computer Vision (ICCV)* pp. 3343–3353 (2021)
- [26] Ryali, C., Hu, Y.T., Bolya, D., Wei, C., Fan, H., Huang, P.Y., Aggarwal, V., Chowdhury, A., Poursaeed, O., Hoffman, J., et al.: Hiera: A hierarchical vision transformer without the bells-and-whistles. *Proceedings of the International Conference on Machine Learning (ICML)* (2023)
- [27] Tulyakov, S., Liu, M.Y., Yang, X., Kautz, J.: Mocogan: Decomposing motion and content for video generation. *Proceedings of the IEEE conference on computer vision and pattern recognition (CVPR)* pp. 1526–1535 (2018)
- [28] Ullah, A., Ahmad, J., Muhammad, K., Sajjad, M., Baik, S.W.: Action recognition in video sequences using deep bi-directional lstm with cnn features. *IEEE Access* **6**, 1155–1166 (2017)
- [29] Viazovetskyi, Y., Ivashkin, V., Kashin, E.: Stylegan2 distillation for feed-forward image manipulation. *Proceedings of the European Conference on Computer Vision (ECCV)* pp. 170–186 (2020)
- [30] Vondrick, C., Pirsivash, H., Torralba, A.: Generating videos with scene dynamics. *Advances in Neural Information Processing Systems* **29** (2016)
- [31] Wang, T.C., Liu, M.Y., Tao, A., Liu, G., Kautz, J., Catanzaro, B.: Few-shot video-to-video synthesis. *arXiv preprint arXiv:1910.12713* (2019)
- [32] Wang, T.C., Liu, M.Y., Zhu, J.Y., Liu, G., Tao, A., Kautz, J., Catanzaro, B.: Video-to-video synthesis. *arXiv preprint arXiv:1808.06601* (2018)
- [33] Xu, J., Anwar, S., Barnes, N., Grimpen, F., Salvado, O., Anderson, S., Armin, M.A.: Ofgan: Realistic rendition of synthetic colonoscopy videos. *International Conference on Medical Image Computing and Computer-Assisted Intervention (MICCAI)* pp. 732–741 (2020)
- [34] Xu, Z., Qi, C., Xu, G.: Semi-supervised attention-guided cycleGAN for data augmentation on medical images. *IEEE International Conference on Bioinformatics and Biomedicine (BIBM)* pp. 563–568 (2019)
- [35] Yang, C., Wang, Z., Zhu, X., Huang, C., Shi, J., Lin, D.: Pose guided human video generation. *Proceedings of the European Conference on Computer Vision (ECCV)* pp. 201–216 (2018)
- [36] Zhu, J.Y., Park, T., Isola, P., Efros, A.: Unpaired image-to-image translation using cycle-consistent adversarial networks. *Proceedings of the IEEE International Conference on Computer Vision (ICCV)* pp. 2223–2232 (2017)